

Journal of Materials Chemistry B

Accepted Manuscript

This article can be cited before page numbers have been issued, to do this please use: S. Brahmachari, M. Ghosh, S. Dutta and P. K. Das, *J. Mater. Chem. B*, 2013, DOI: 10.1039/C3TB21334J.



This is an *Accepted Manuscript*, which has been through the RSC Publishing peer review process and has been accepted for publication.

Accepted Manuscripts are published online shortly after acceptance, which is prior to technical editing, formatting and proof reading. This free service from RSC Publishing allows authors to make their results available to the community, in citable form, before publication of the edited article. This *Accepted Manuscript* will be replaced by the edited and formatted *Advance Article* as soon as this is available.

To cite this manuscript please use its permanent Digital Object Identifier (DOI®), which is identical for all formats of publication.

More information about *Accepted Manuscripts* can be found in the [Information for Authors](#).

Please note that technical editing may introduce minor changes to the text and/or graphics contained in the manuscript submitted by the author(s) which may alter content, and that the standard [Terms & Conditions](#) and the [ethical guidelines](#) that apply to the journal are still applicable. In no event shall the RSC be held responsible for any errors or omissions in these *Accepted Manuscript* manuscripts or any consequences arising from the use of any information contained in them.

Biotinylated amphiphile-single walled carbon nanotube conjugate for target-specific delivery to cancer cells

Sayanti Brahmachari, Moumita Ghosh, Sounak Dutta, and Prasanta Kumar Das*

*Department of Biological Chemistry, Indian Association for the Cultivation of Science,
Jadavpur, Kolkata – 700 032, India*

*To whom correspondence should be addressed. Fax: +(91)-33-24732805, E-mail: bcpkd@iacs.res.in

Abstract

The present work reports specific targeting of cancerous cells using non-covalently water dispersed nanoconjugate of biotinylated amphiphile-single walled carbon nanotube (SWNT). The fundamental approach involves incorporation of the biotin into the architecture of the carbon nanotube (CNT) dispersing agent to develop a multifaceted delivery vehicle having high colloidal stability, substantial cell viability and target specificity towards cancer cells. A three way functionalization strategy has been employed to introduce a C-16 hydrophobic segment, polyethylene glycol hydrophilic fragment and biotin as the target-specific unit at the -OH, -COOH and -NH₂ terminals of L-tyrosine, respectively. The newly developed neutral amphiphile exhibited efficient SWNT dispersion (72%) in water, significant viability of different mammalian cells (Hela, HepG2, CHO and HEK-293) up to 48 h and also media stability. Most importantly, the biotinylated amphiphile-SWNT dispersion successfully transported the fluorescently labelled Cy3-oligoneucleotide (loaded on the surface of CNT) inside the cancerous Hela, HepG2 cells after 3 h of incubation in contrast to CHO and HEK-293 cells (devoid of overexpressed biotin receptors). The presence of biotin moiety in the cellular transporters facilitated the internalization of cargo due to the overexpressed biotin receptors in cancer cells. Importantly, this nanohybrid was also capable of specifically transporting anticancer drug doxorubicin to cancer cells that led to the significant killing of Hela cells compared to the normal CHO cells. Thus, receptor-mediated specific transportation of cargo into cancer cells was possible only due to the biotinylated CNT dispersing agent. To the best of our knowledge this is the first reported amino acid based biotinylated small amphiphilic molecule that non-covalently dispersed SWNT and the corresponding nanoconjugate showed excellent cell viability, antibiofouling property and desired target-specific drug delivery.

Introduction

In the last decade, the uses of carbon allotropes in several frontiers of research have gained significant importance owing to its unique physical, electronic and optical properties.¹ Amongst others, SWNT being endowed with cylindrical structure and high aspect ratio have emerged with enormous promise in nanobiotechnology.² Of late substantial efforts have been made for the engineering of multifaceted nanosystems capable of serving as efficient diagnostic and therapeutic tools.³ In fact the ability of SWNT to translocate through cell membrane and its chemical inertness make this carbon nanomaterial highly promising in the quest of developing cutting edge drug delivery vehicle. The huge surface area of SWNT is considered to be ideal for uploading cargo at higher concentration, which can assist in improving the bioavailability and effectiveness of relevant molecules.⁴ However, the first step to utilize these nanomaterials in biomedical applications involves its solubilization in the biological milieu. In order to solubilize SWNTs, exogenous capping units have been attached to the side-walls and these functional units primarily govern the properties of the dispersions.⁵ Hence, proper exploitation of the SWNTs in the biomedical arena lies in the design and functionality of the inducted motifs within dispersing agents.

The designed nanocarriers must satisfy several prerequisites for their effective utilization as cellular transporters. Firstly (i) the SWNT needs to be sufficiently dispersed in water, (ii) the aqueous SWNT dispersion must be satisfactorily viable to mammalian cells, (iii) preferably it should exhibit stealth properties to escape the immune system, and (iv) suitable ligands need to be fringed in order to achieve the “active targeting” to specific cells or tissues. Till date SWNT dispersion has been achieved using various small molecules like surfactants as well as by macromolecules like polymers and proteins.⁶ To this end, recently we reported the efficient SWNT dispersion and successful delivery of proteins inside

mammalian cells using SWNT-amphiphile (comprising of L-alanine and polyethylene glycol (PEG), Fig. S1, Electronic Supplementary Information (ESI)) composite as vectors.⁷ PEG moiety is normally integrated within the dispersing agent or at the side wall of nanotube with the aim to improve the cell viability of SWNT dispersion as well as to impart stealth properties within the developed hybrids.⁸

The other challenging hurdle for any delivery system is target-specific cellular transportation. Till date quite a few tumour targeting ligands are known that are integrated within the designed delivery systems.⁹ Delivery vehicle equipped with tumor-targeting ligands recognize the overexpressed cancer-specific receptors on the cell surface and thereby specifically internalized within cancerous cells. Some typical tumor-targeting motifs include polysaccharides like hyaluronic acid, monoclonal antibodies, polyunsaturated fatty acids, EGF (epidermal growth factor), peptide like RGD and vitamins like folic acid and biotin.^{9a} The CNT-based delivery systems are gaining more significance in this line of research by the inclusion of target-specific ligand on its surface. Among all the known targeting markers, exploration on the specificity of biotin has received comparatively little attention.¹⁰ Biotin is an essential vitamin for the growth of all cells but the demand for this vitamin is considerably higher in the rapidly dividing cells and tissues. Biotin receptors are even more overexpressed than the folate receptors in many cancer cells.¹¹ In this regard, Ojima and co-workers reported the specific delivery of fluorophore tagged SWNT covalently functionalized with biotin to L1210FR cells.^{9a} Thus, designing of dispersing agents, which are cell viable, antibiofouling as well as target-specific towards cancerous cells deserve considerable attention as cellular transporters.

In the present manuscript we report efficient aqueous dispersion of SWNT using newly designed biotinylated amphiphile comprising of tyrosine, PEG moiety and C-16 alkyl chain (**1**, Scheme 1). Biotin was integrated in the architecture of the amphiphilic dispersing

agent to achieve specificity towards cancerous cells (Fig. 1). The well dispersed nanotubes were characterized using spectroscopic and microscopic techniques. Subsequently the cell viability and media stability in the biological milieu was ensured. The developed biotinylated amphiphile-SWNT dispersions facilitated the specific transportation of fluorescently labelled oligonucleotide into different cancerous cells (cervical cancer derived Hela cells and Human hepatic cancer derived HepG2) in contrast to non-cancerous Chinese Hamster Ovarian (CHO) and Human embryonic Kidney (HEK-293) cells.¹² Most interestingly, targeted killing of cancer cell was achieved by the specific delivery of doxorubicin loaded on this newly developed nanoconjugate into Hela cells.

Results and discussion

Synthesis of SWNT-dispersing agent

A common approach to disperse CNTs in water involves non-covalent functionalization of CNTs with small amphiphilic molecules.⁵ In general the hydrophobic end of molecule binds to the SWNT surface while the hydrophilic part remains oriented towards the aqueous domain. To this end we have recently reported the synthesis of amphiphilic dispersing agents, comprising of L-alanine or L-phenyl alanine linked to a C-16 alkyl chain and a PEG unit at the hydrophilic terminal (Fig. S1, ESI).⁷ The SWNT debundling efficiency of those PEG containing amphiphiles was about 85%. However these nanoconjugates transported fluorescently labelled proteins into both HepG2 cells and CHO cells with equal efficiency. Therefore, despite being an efficient delivery system, these nanohybrids lack specificity between cancerous and non-cancerous cells.

Hence the primary aim of this work is to synthesize a SWNT dispersing agent which can exhibit significant stability in biological media, high cell viability and target specificity towards cancer cells. Thus inclusion of an additional target-specific moiety in the structure of

dispersing agent is required along with the presence of hydrophobic and hydrophilic segments. With this aim we choose naturally occurring L-tyrosine as the molecular core where three way functionalizations can be carried out to synthesize desired dispersing agent, **1**. Firstly the C-16 alkyl chain (hydrophobic/lipophilic segment) was incorporated at the phenolic –OH terminal by the substitution reaction using corresponding alkyl bromide (Scheme 1). Followed by the COOH terminal of the amino acid was coupled with the PEG (550) unit through DCC coupling. The targeting biomarker, biotin was converted to the corresponding active ester using *N*-hydroxy succinimide (NHS). This activated intermediate (NHS-biotin) subsequently reacted with the –NH₂ end of the amino acid in presence of dry pyridine to synthesize the amphiphilic SWNT dispersing agent, **1**.

SWNT dispersion and characterization

The SWNT dispersing ability of **1** was tested following the previously reported protocol.^{6h} About 1 mg of pristine SWNT was taken in 4 mL aqueous solution of **1** (2.5 mg/mL) and sonicated by both probe and bath sonicator. It was subsequently centrifuged at 2500 g for 90 min to remove the heavier bundled CNTs. The supernatant solution contained dispersed nanotubes and this SWNT-**1** dispersion remained stable for months. The amount of SWNT in the dispersed state was determined from the calibration plot previously prepared using SDBS.^{6h,13} The amphiphile **1** efficiently dispersed SWNT (72%) in water. The van der Waals interaction between the long alkyl chain of **1** and the SWNT possibly facilitated the anchoring of former onto the nanotube walls while the hydrophilic PEG unit oriented towards the hydrophilic domain helped in exfoliation of the CNTs by steric repulsion.¹⁴ The hydrogen-bonded water molecules also hinder the re-aggregation and precipitation of the nanotubes. In order to determine the percentage of amphiphile interacting with the nanotubes and involved in the process of dispersion, the obtained supernatant was centrifuged at 375000 g. The supernatant was discarded and the palette was subjected to Thermogravimetric

Analysis (TGA) (Fig. S2, ESI). The sharp decrease in weight between 200-400 °C corresponds to the decomposition of the amphiphile. About 25% residue remains after the decomposition indicating the amount of SWNT present in the sample. Hence ~ 75% of the used amphiphilic dispersing agent gets attached to the walls of SWNT.

The stability of any colloidal system is primarily governed by- i) the repulsive force acting between the particles and ii) the attractive van der Waals attraction that leads to coagulation and precipitation. The zeta (ζ)-potential study of a colloidal system has been extensively used in the literature to determine the stability of such colloidal systems. The ζ -potential provides a good insight into the interplay of the various forces and the overall stability of the dispersed nanohybrids in solution.^{6h,14} The ζ -potential of SWNT-1 was found to be -18.9 mV. In general colloidal solutions having ζ -potential values above and below ± 15.5 mV is considered to be a stable solution.^{6h,14} High ζ -potential values for SWNT dispersions are mostly observed where electrostatic interactions are playing a dominating role on the stability of colloids. Nonetheless, even in the absence of any such charge bearing unit, the high ζ -potential value for SWNT-1 indicates high stability of the debundled nanotubes possibly due to the repulsive forces between individual nanotubes that was originated from the steric bulk of the PEG unit.¹⁴ Also the hydrogen bonding of oxygen-containing glycol chain with water molecules might have prevented the coagulation of the SWNT-amphiphile nanohybrids and facilitated its homogenous dispersion in water.

Characterization of the aqueous dispersion of SWNT-amphiphiles was further done by UV-vis-NIR spectroscopy. Discernable peaks were observed both in the range of 550-900 nm (S_{22} transition) and 800-1600 nm (S_{11} transition) for the aqueous dispersion of SWNT-1 (Fig. 2a).^{5d,m,6h,15} The distinct peaks due to the interband transitions (S_{22} and S_{11}) between the mirror image spikes in the density of states of the SWNTs indicate well exfoliation of nanotubes in water and the unperturbed electronic structure of SWNT. The SWNT dispersion

was also examined by transmission electron microscopy (TEM). The TEM images of SWNT-1 revealed highly dispersed nanotubes having an average diameter of 5 nm (Fig. 2b). Additionally the quality of dispersion was studied using atomic force microscopy (AFM) (Fig. 2c) and histograms were prepared to estimate the dimension of the dispersed nanotubes.^{5m,7} The average diameter of the dispersed nanotubes was between 5-6 nm while the average length was between 400-500 nm (Fig. S3, S4, ESI). Both spectroscopic and microscopic investigations confirmed the efficient debundling of SWNT in water by the newly designed amphiphile 1.

Cell viability and stability

The issue of cell viability is an extremely basic prerequisite that needs to be confirmed while designing any kind of delivery system. Having ensured the quality and quantity of SWNT-1 dispersion, the next important issue was to examine the cell viability of this nanohybrid. The cell viability of SWNT-1 was tested against HEK-293, CHO, Hela and HepG2 cells using MTT assay. The different cells were incubated for 48 h with varying concentration of SWNT-1 and interestingly almost 85% cells were viable after 48 h of incubation up to 25 $\mu\text{g/mL}$ of SWNT-1 (Fig. 3a). Encouragingly, when the concentration of the nanohybrid increased to 50 $\mu\text{g/mL}$, the cell viability was still considerably high, 81% in case of Hela, 85% in HepG2, 81% in HEK-293 and to 80% in case of CHO cells. Hence the newly developed nanohybrid is inferred to be satisfactorily cell viable.

In addition to the cell viability, the SWNT based biological transporter must have substantial stability in the biological milieu particularly in presence of high salt and protein content.⁸ The stability of colloidal suspension depends on the balance between the attractive van der Waals force and the repulsive electrostatic force.¹⁴ Aggregation induced coagulation and precipitation of the nanomaterials in the biological fluid is a common occurrence and that often leads to the blocking of capillaries. The instability of colloidal nanoparticles arises due

to nonspecific adsorption of proteins and consequently the replacement of the dispersing agent resulted in the precipitation of nanomaterials.^{4b,8a} High salt and protein content of the blood plasma may become a major obstacle towards actual implementation of the colloidal delivery system.^{1a,8,16} The stability of the newly developed nanohybrid was visually assessed in phosphate buffer saline (PBS) with increasing ionic concentrations (0-150 mM) for 48 h using 25 $\mu\text{g/mL}$ of SWNT-1. Notably, the nanoconjugate was found to be highly stable (Fig. 3b) even at 150 mM concentration of PBS. The suspension stability index (SSI) (details given in ESI) of all the incubations was measured and no decrease in the value was observed after 48 h of incubation (Fig. S5, ESI). The uncharged hydrophilic PEG unit with its steric bulk presumably hinders the formation of electrical double-layer on the surface of the colloidal particles that is known to reduce the repulsive forces.¹⁴

Furthermore we tested the stability of SWNT dispersions in serum mimicking compositions having cell culture media (DMEM) and varying concentration of fetal bovine serum (FBS) protein. It is known that non-specific adsorption of biological components of plasma on nanotube surface particularly in case of non-covalent CNT-dispersion, could result in the uptake of the foreign materials by the macrophages of the reticuloendothelial system (RES).^{1a,8,16} Thus, SWNT-1 (25 $\mu\text{g/mL}$) was incubated in DMEM media containing FBS (0-100%) protein for 48 h under sterile condition. Encouragingly, no precipitation of the nanomaterial was observed even when the protein concentration was increased to 100% FBS (Fig. 3c). Additionally the SSI of the solutions was found to be above 90% for all the solutions after 48 h (Fig S6, ESI). Again the neutral PEG unit possibly acts as a protection layer around the colloidal entities because of having hydration around itself (stealth character) and resists direct interaction of the proteins and ions with the nanomaterial in the biological system.^{4b,8a,e,f} These observations also indicate that the attachment of the amphiphilic dispersing agent (**1**) on SWNT surface is highly stable and chances of surfactant

exchange in the blood plasma is very poor. Furthermore circulation of nanoconjugate within body fluids is also essential for the sustained delivery of cargo inside the cells. To this end, stability of SWNT-1 (25 $\mu\text{g/mL}$) was also investigated for ten days in 10% FBS-DMEM culture media (condition normally used for the proliferation of cells). SWNT-1 dispersion was found to be stable for the entire period of time and SSI was above 95% at the end of ten days (Fig. S7, ESI). This highly dispersed SWNT-1 nanoconjugate along with its considerable cell viability and remarkable stability in biological milieu meets all the essential criteria that required for a cellular transporters.

Oligonucleotide loading on dispersed SWNT

The loading capacity of the nanohybrid was investigated prior to its utilization as cellular transporters. 15-mer oligonucleotide = ACCTGTGAGCCTTAC (Olg) was chosen as the cargo and the percentage of oligonucleotide loaded on to SWNT-1 surface was calculated using agarose gel electrophoretic study. The complexation of oligonucleotide with SWNT inhibits the intercalation of ethidium bromide (EtBr) with the oligonucleotide thereby EtBr cannot exhibit any fluorescence emission. Hence it is not possible to visualise the complexed oligonucleotide with SWNT, instead the free oligonucleotide was estimated to calculate the loading capacity of the nanoconjugates.¹⁷ The migration behaviour of the different SWNT-1-Olg composites (having varied concentration ratio of SWNT-1 to oligonucleotide) was studied against uncomplexed oligonucleotide (30 μM) (Fig. 4a,b). The observed fluorescent band in lane 1 originated due to the intercalation of EtBr with the free oligonucleotide and other three lanes (2 to 4) were loaded with same amount of oligonucleotide premixed with 25, 50 and 100 $\mu\text{g/mL}$ of SWNT-1, respectively (Fig. 4a). In order to quantify the fluorescence intensity of EtBr intercalated with unbound oligonucleotide, densitometric analysis was carried for the luminescent zone (black region just above the luminescent zone in each lane was due to the presence of bromophenol blue). Sequential decrease in the fluorescence

intensity from lane 2 to 4 indicates a decrease in the amount of available free oligonucleotide or increase in the complexed oligonucleotide with increase in the concentration of nanoconjugate (Fig. 4a,b). It was found almost 75% oligonucleotide remained in the unbound state when 25 $\mu\text{g/mL}$ SWNT-1 was incubated with 30 μM oligonucleotide i.e. 25% of the cargo (7.5 μM) was loaded on to the nanotube surface. The percentage of loaded oligonucleotide sequentially increased to 31 and 45% when the concentration of SWNT-1 was increased to 50 and 100 $\mu\text{g/mL}$, respectively.

The loading of oligonucleotide onto the nanotubes was also studied using fluorescence spectroscopy. For this purpose a stock solution (1.25 μM) of fluorescently labelled oligonucleotide (Cy3-ACCTGTGAGCCTTAC = Cy3-Olg) was prepared in water and the fluorescence spectrum of this solution exhibited maximum emission at 565 nm (Fig. 4c) upon exciting the probe at 550 nm. Hereafter SWNT-1 (50 $\mu\text{g/mL}$) was mixed with this Cy3-Olg solution for 4 h to load the oligonucleotide on the surface of dispersed nanotubes. The aqueous dispersion was centrifuged at 175000 g to precipitate out the Cy3-Olg loaded SWNT-1. The fluorescence spectrum of the supernatant was then recorded which showed significant drop in the emission intensity compared to that of native Cy3-Olg (Fig. 4c). This dramatic decrease in the emission intensity clearly suggests the absence of free Cy3-Olg in the supernatant solution. Therefore almost complete loading of Cy3-Olg has taken place on the surface of nanotube leading to the formation of SWNT-1-Cy3-Olg nanobioconjugate. We also estimated the amount of loaded cargo on the nanovectors by using the UV-vis absorption of Cy3-Olg at 540 nm. A calibration plot of Cy3-Olg was prepared by sequential dilution of its stock solution (Fig S8, ESI). The conjugate was then prepared by incubating 50 $\mu\text{g/mL}$ SWNT-1 with 1.25 μM Cy3-Olg for 4 h. The hybrid was centrifuged and washed twice at 175000 g till no unbound oligonucleotide was present in the supernatant. The obtained palette was re-dispersed in 1 wt % (w/v) of SDS solution and sonicated. The dispersed

solution was again centrifuged and the supernatant was collected. The absorbance was measured and the concentration of the Cy3-Olg in the supernatant was found to be 1.12 μM . The addition of the anionic surfactant SDS led to the removal of the bound oligonucleotide from the surface of the nanotubes which resulted in the increased absorbance of the supernatant.^{17b} Thus the experiment further showed almost complete loading of the oligonucleotide on the nanotube surface.

Target-specific cellular internalization

After ensuring the cell viability, media stability and loading capacity of the SWNT-1 nanohybrid, the vector was used for transporting the fluorescent probe labelled Cy3-Olg inside the mammalian cells. Cy3-Olg was non-covalently loaded onto the surface of dispersed nanotubes by stirring the oligonucleotide in the aqueous dispersion of SWNT-1 in dark for 4 h (see experimental section for details). The cargo loaded nanocomposites were then incubated with cancerous HeLa and HepG2 cells for 3 h at 37 °C in 5% CO₂ atmosphere. Both cells have overexpressed biotin receptors on their surface.^{3a,9a,10,11b,c} The typical concentration of the delivering unit (SWNT-1) was 10 $\mu\text{g/mL}$ and that of the cargo (Cy3-Olg) was 0.25 μM . In accordance with the binding affinity pattern of oligonucleotide towards the dispersed SWNT-1 (Fig. 4), it is expected that almost complete loading of oligonucleotide has taken place on the surface of SWNT. The incubation was followed by washing of the cells with PBS buffer in order to remove the excess conjugate from the medium. Encouragingly, successful internalization of oligonucleotide inside the cancerous cells by SWNT-1 was evident from the highly intense red fluorescence microscopic images (Fig. 5a-b, d-e) of HeLa and HepG2 cells. Also the corresponding flow cytometric analysis of the cancerous cells further confirmed the successful internalization of Cy3-Olg inside cancerous cell (Fig. 5c,f). The healthy nature of the cells was ascertained from their spindle shape in the corresponding bright field images. The viability of the cells was confirmed by incubating both HeLa and

HepG2 cells with 10 $\mu\text{g}/\text{mL}$ SWNT-1 for 3 h followed by treating with the LIVE/DEAD viability kit (Fig. S9 a,b,d,e, ESI). The predominant presence of green cells and absence of red cells in fluorescence images further validated the existence of living cells as well as significant cell viability of the nanohybrid. The cell viability was also studied using flow cytometry (Fig S9 c,f) where the significant presence of green cells and clear absence of red stained cells indicate the healthy nature of the cells. The self-internalization ability of Cy3-Olg (0.25 μM) alone within HeLa and HepG2 cells in absence of SWNT-1 was studied keeping other experimental conditions same (details given in ESI). Absence of almost any red fluorescent cells confirmed the inability of self-internalization of Cy3-Olg without the assistance of nanoconjugate (Fig. S10, ESI). The flow cytometric analysis also confirmed the poor self internalisation ability of the cargo (Fig. S11, ESI). The transportation ability of the amphiphilic dispersing agent (**1**) through formation of any supramolecular aggregate was also investigated. For this purpose the critical micellar concentration (CMC) of **1** was measured tensiometrically and it was found to be 14.3 $\mu\text{g}/\text{mL}$ (Fig. S12, ESI). The solutions of **1** (10 $\mu\text{g}/\text{mL}$) and (50 $\mu\text{g}/\text{mL}$) was mixed with Cy3-Olg (0.25 μM) and incubated with HeLa and HepG2 cells under identical experimental conditions for 3h at 37 $^{\circ}\text{C}$. The amphiphile concentration was kept well above and below the CMC to ascertain the presence and absence of its self-aggregated structure during the experiment. However, no significant internalization of the fluorescent labelled oligonucleotide was observed (Fig. S13, ESI). The above observation was also confirmed using flow cytometric experiments and the low mean fluorescence intensity indicated the poor internalisation ability of the cargo by formation of other supramolecular aggregates (Fig S11, ESI). Hence, SWNT-1 nanoconjugate exclusively transported the cargo inside the cancer cells.

At this point, the most crucial issue is to investigate the specificity of SWNT-1 towards cancerous cells. The specificity of the developed nanohybrid was evaluated by

investigating the cargo delivery ability of SWNT-1 into CHO cells and HEK-293 cells, devoid of overexpressed biotin receptors. Similar to the preceding experiments for cancerous cells, here also Cy3-Olg (0.25 μ M) loaded SWNT-1 (10 μ g/mL) was incubated with CHO cells and HEK-293 cells for 3 h at 37 $^{\circ}$ C. Almost complete absence of red fluorescent cells in the corresponding microscopic image (Fig. 5g,h,j,k) confirmed the non-delivery of Cy3-Olg into these cells. Similarly, the corresponding flow cytometry data showed poor fluorescent intensity (Fig. 5i,l). Thus the extent of delivery of the oligonucleotide in normal cells was significantly lower than that was observed for HeLa and HepG2 cells. Moreover, the receptor-mediated specific transportation of cargo in cancerous cells was examined by pre-treating the cells with ligand. The HeLa cells were pre-incubated with biotin solution (2 mM) for 1 h and these treated cells were incubated with the Cy3-Olg loaded SWNT-1 for 3 h at 37 $^{\circ}$ C.^{9a} The extent of cargo internalization was notably lower as observed in the microscopic images (Fig. 5,m,n) compared to that was observed for biotin-untreated HeLa cells. Corresponding flow cytometry data affirmed the decreased cargo internalisation in the treated cells (Fig 5o). The pre-treatment with the ligand probably led to the blocking of the overexpressed receptors in the cancer cells resulting in the reduced internalization. Also the extent of delivery was checked in HeLa cells using the Cy3-Olg loaded SWNT dispersed by previously reported PEGylated-amino acid based amphiphile (Fig S1, ESI) devoid of biotin. Interestingly the corresponding fluorescence image and the flow cytometry data revealed significantly lower transportation after 3 h of incubation (Fig 5 p-r). The target-specific transportation takes place due to the presence of overexpressed biotin receptors in the rapidly dividing cancerous cells and tissues.^{3a,9a,10,11} Thus, the overexpression of biotin receptors on HeLa and HepG2 cells surface and lack of the same on CHO cell and HEK-293 cell made the biotinylated amphiphile-SWNT nanohybrid target-specific toward cancerous cells.

The cargo internalization experiments for Cy3-Olg loaded SWNT-1 were again carried out in CHO cells and HEK-293 cells at a longer time scale (from 6 to 48h). However after 48 h of incubation, detectable delivery of cargo was observed into CHO cells and HEK-293 cells (Fig. S14,a,b,d,e, ESI). The similar pattern of uptake is also evident from the enhanced fluorescence intensity in the flow cytometry data of CHO and HEK-293 cells after 48 h of incubation (Fig S14, c,f). Hence, SWNT-1 hybrid has at least 48 h specificity towards Hela and HepG2 cancerous cells compared to that of CHO cells and HEK-293 cells. The viability of the CHO and HEK-293 cells were also examined using LIVE/DEAD viability kit after 48 h of incubation with SWNT-1. Here too, the absence of red cells and presence of green cells affirmed the substantial viability of the mammalian cells (Fig. S15,a,b,d,e, ESI). Almost complete absence of red cells was also confirmed from the flow cytometry (Fig S15 c,f, ESI). Thus by way of rational designing we have been able to develop simple surfactant based efficient SWNT dispersing agent, which is significantly biocompatible and has achieved target-specific transportation of biomolecules into cancerous cells.

Internalization pathway mechanism

In view of the successful target-specific transportation of biomolecule into cancerous cells by biotinylated amphiphile-SWNT dispersion we were curious to investigate the mechanism of internalization. The exact mechanism of cellular internalization of SWNT is still a matter of serious debate.^{9a} The two mostly discussed mechanisms of cellular uptake are i) CNT act as nanoneedles and pierce through the cell membrane and (ii) the other mechanism involves endocytotic pathway. Generally, the former is an energy independent process while the latter is energy dependent process, which is hindered at low temperature or in the presence of a metabolic inhibitor, such as NaN_3 . To probe the mechanism of uptake, cellular transportation was carried out under energy depleted condition keeping all other experimental conditions identical (details given in SI). Hela cells were pre-treated with 10 mM solution of NaN_3 for

30 min to ensure energy depleted condition. This was followed by incubation of those cells with 10 $\mu\text{g}/\text{mL}$ SWNT-1-Cy3-Olg (0.25 μM) for 3 h at 37 $^{\circ}\text{C}$. Microscopic imaging of the cells revealed significant decrease in the nanoconjugates uptake (Fig. S16 a,b, ESI) since no detectable red fluorescent cell was observed. Similarly, Hela cells were incubated with the same SWNT-1-Olg for 3 h at 4 $^{\circ}\text{C}$ instead of 37 $^{\circ}\text{C}$ and the very poor intensity of red fluorescence in microscopic images delineated substantial drop in the internalization of nanohybrid (Fig. S16,d,e, ESI). The flow cytometric analysis also indicated the poor transportation of the oligoneucleotide under energy depleted conditions (Fig S16, c,f). The viability of the cells after treatment with NaN_3 was checked using LIVE/DEAD assay and the predominance of green cells indicated the presence of live cells (Fig. S17,a,b ESI). The flow cytometric analysis also confirmed the viability of the azide treated cells (Fig S17 c, ESI). Hence the biological transportation by SWNT-1 predominantly followed the energy dependent receptor-mediated endocytotic pathway.

This biological transportation of oligonucleotide inside cancer cell by SWNT-1 was further studied by nucleus staining experiments. This was done to counter stain the nucleus and clearly demarcate the cytoplasm from the nucleus of cell. The Cy3-Olg internalized Hela cells were subsequently incubated with nucleus staining agent Hoechst dye (2.5 $\mu\text{g}/\text{mL}$) for 30 min. The blue colour originates from the intercalation of Hoechst dye into the nuclear oligonucleotide (Fig. 6a) and the red coloured region corresponds to the already internalized Cy3-Olg (Fig. 6b). The dual colour in the superimposed image (Fig. 6c) clearly showed the accumulation of red Cy3-Olg in the cytoplasmic region and blue Hoechst dye in the nucleus with little co-localization of Cy3-Olg. However after 24 h incubation of SWNT-1-Cy3-Olg with Hela cells, microscopic images clearly revealed significant localization of the cargo inside the nucleus (Fig. S18, ESI), which was also supplemented by nucleus staining

experiments. Thus, this newly developed nanovector can also be utilized for targeted gene/drug delivery in biotin overexpressed cancer cells.

Target-specific drug delivery

Receptor-mediated successful delivery of oligonucleotide into cancerous cells prompted us to utilize this newly developed nanovector for clinically important targeted drug delivery to cancer cells. For this purpose a well known anticancer drug, doxorubicin was chosen. The poor solubility and lack of specificity are some of the primary problems associated with the drug administration. Hence with the aim of target-specific delivery of doxorubicin to cancer cells, the drug was hydrophobically loaded onto the walls of the nanohybrid (SWNT-1). This was done by overnight incubation of the drug with 100 $\mu\text{g/mL}$ SWNT-1 in pH 8.0 (PBS buffer) to maintain an optimal weight ratio of 2:1 (SWNT:doxorubicin).¹⁸ The loading of the drug was ensured from the UV-vis absorbance spectra where doxorubicin itself exhibits a UV-Vis absorbance maxima at 492 nm (Fig. 7a). Upon loading of this chromophoric drug on SWNT surface, a new peak was observed for the SWNT-1-DOX hybrid having an absorbance maxima at 502 nm, which was absent in the spectra of the SWNT alone.¹⁸ This red shifted peak of doxorubicin in the hybrid material clearly indicates its interaction with the walls of the nanotube and loading of the same.^{18b,gj} To further ensure the loading of doxorubicin on the surface of nanohybrid, the photoluminescence spectra of the drug were recorded (Fig. 7b). The spectrum of free doxorubicin showed an emission maximum around 600 nm upon excitation at 490 nm. Interestingly, almost complete quenching of this peak was noted for the drug loaded SWNT-1 composite indicating the absence of free doxorubicin in the sample.^{18a} Thus the SWNT backbone of the nanovector allowed the binding of the drug possibly through interaction between aromatic groups and efficient loading of the doxorubicin took place leading to the formation of the target-specific vector, SWNT-1-DOX.

The loading of doxorubicin was further confirmed by measuring the amount of released doxorubicin at low pH. The drug is known to have higher hydrophilicity at lower pH due to the protonation of the $-NH_2$ leading to lower affinity towards hydrophobic SWNT surface.^{6j} The chromophoric drug exhibits a maxima in its UV-vis spectra at 490 nm hence a calibration plot was prepared by sequential dilution at 470 nm (Fig S19, ESI). Doxorubicin (50 $\mu\text{g}/\text{mL}$) was loaded onto the surface of the nanotube by incubating with 100 $\mu\text{g}/\text{mL}$ SWNT-1 at pH 8.0 buffer. The conjugate was centrifuged at 175000 g to remove the unbound doxorubicin and the obtained palette was re-dispersed in 1 N HCl to detach the loaded doxorubicin. The solution was again centrifuged and the amount of doxorubicin released in the supernatant was found to be 46 $\mu\text{g}/\text{mL}$. Hence the study vividly showed almost complete the loading of the drug on the surface of dispersed SWNT.

The targeted drug delivery of doxorubicin by this nanohybrid (SWNT-1) was then examined by the incubation of cancerous Hela cells and non-cancerous CHO cells with the SWNT-1-DOX for 12 h. The concentration of SWNT-1-DOX was varied over a range and the maximum concentration of the drug was kept at 10 $\mu\text{g}/\text{mL}$ and that of the vector SWNT-1 was at 20 $\mu\text{g}/\text{mL}$. The percentage of live cells after the incubation was determined using MTT assay and encouragingly a marked difference in the killing efficiency was observed. At 2.5 $\mu\text{g}/\text{mL}$ of doxorubicin and 5 $\mu\text{g}/\text{mL}$ of SWNT-1, 92% CHO cells were alive while only 46% Hela cells were found to be dead (Fig. 7c). Importantly, when the concentration of the hybrid was increased to 10 $\mu\text{g}/\text{mL}$ of doxorubicin and 20 $\mu\text{g}/\text{mL}$ of SWNT-1, more than 60% Hela cells were killed in contrast to that of only 15% for CHO cells. Alongside, the efficiency of native doxorubicin was tested and it was observed that the drug alone had very poor killing efficiency. Almost 80% Hela cells and 85% CHO cells were alive when 10 $\mu\text{g}/\text{mL}$ drug was incubated for 12 h and the IC_{50} (Half Inhibitory Concentration) was $>10\mu\text{g}/\text{mL}$ (Fig S20, ESI). Most interestingly this IC_{50} value decreased to 7.5 $\mu\text{g}/\text{mL}$ when the drug was used in

combination with SWNT-1. Also the marked difference in the killing ability of doxorubicin between HeLa and CHO cells can only be attributed to the target-specific drug delivery by SWNT-1 induced by the tumour targeting agent, biotin.

Conclusion

In summary, the present work described a simple approach to develop a SWNT based cellular delivery vector in combination with amino acid based biotinylated amphiphile. The spectroscopic and microscopic studies indicate the superior dispersing ability of the newly developed amphiphilic dispersing agent. This amino acid based amphiphile comprising of a PEG unit ensured the low cytotoxicity and significant stability in media containing varying concentration of salt and protein. Most encouragingly the incorporation of biotin in the amphiphile's structure facilitated the specific delivery of Cy3-Olg and doxorubicin loaded SWNT-1 conjugate into cancerous cells due to the overexpressed biotin receptors in these rapidly dividing cells. Thus by way of rational designing of amphiphilic molecule we have achieved target-specific delivery of biomolecule and drug into cancerous cells using non-covalently modified SWNT. Such 'specific-targeting' model can be used to develop effective delivery platforms in biomedicine.

Materials and Methods

Materials

Silica gel of 60-120 mesh, L-tyrosine, cetyl bromide, *N,N*-dicyclohexylcarbodiimide (DCC), 4-*N,N*-(dimethylamino)pyridine (DMAP), 1-hydroxybenzotriazole (HOBT), D-biotin, sodium dodecylbenzene sulfonate, *N*-hydroxysuccinimide (NHS), pyridine, dimethyl formamide (DMF), agarose for gel electrophoresis, ethidium bromide, solvents and all other reagents were procured from SRL, India. thionyl chloride, and sodium hydroxide were purchased from Spectrochem, India. Glycerol was obtained from Merck. Water used

throughout the study was Milli-Q water. Single walled carbon nanotubes (SWNT, 1.2-1.5 nm diameter), CDCl_3 for NMR experiments, polyethylene glycol (PEG, $M_n = 550$) and bromophenol blue, sodium azide were obtained from Aldrich Chemical Co. The LIVE/DEAD® viability kit (L-3224) for eukaryotic cells, Dulbecco's Modified Eagles' Medium (DMEM), heat inactivated fetal bovine serum (FBS), Hoechst dye, trypsin from porcine pancreas and penicillin-streptomycin was procured from Molecular Probes, Invitrogen Chemical Company. Thiazolyl blue tetrazolium bromide (MTT), Cy3 labelled oligonucleotide and oligonucleotide were obtained from Sigma Aldrich Chemical Company. Perkin Elmer Lambda 25 spectrophotometer was used to record the UV-VIS spectra while the UV-Vis-NIR spectra were monitored using Varian Cary 5000 spectrophotometer. ^1H NMR spectra were recorded in an AVANCE 500 MHz (Bruker) spectrometer. Fluorescence emission spectra were recorded in Varian Cary Eclipse Luminescence spectrometer at excitation and emission slit widths of 2.5 nm. Transmission Electron Microscopy (TEM) measurements were performed on JEOL JEM 2010 microscope. Atomic force microscopy (AFM) was performed on Veeco, model AP0100 microscope in non-contact mode. Probe sonication was done using Omni Sonic Ruptor 250. Bath sonication was performed with a Telsonic Ultrasonics bath sonicator. Sorvall RC 6 and Sorvall RC 90 were used for centrifugation and ultracentrifugation, respectively. Bio Rad Gel Doc XR was used for the imaging of agarose gels. Olympus IX51 inverted microscope was used for imaging of the cells. Cell-associated fluorescence was monitored on fluorescence activated cell sorter (FACS) Calibur flow cytometer (Becton Dickinson, San Jose, CA) with the excitation wavelength at 560 nm.

Synthesis of 1

Complete synthetic procedure and reagents are delineated in Scheme 1. At first the -COOH terminal of L-tyrosine was esterified using thionyl chloride in methanol. The methyl ester

protected amino acid was then taken in DCM and drop wise BOC-anhydride was added in the presence of triethylamine. The reaction mixture was then taken in ethyl acetate (EtOAc) and washed well with 1 N HCl to remove the free amine. The organic layer was then washed to neutrality using brine and evaporated to get the Boc-protected methyl ester of L-tyrosine (**I**). The intermediate, **I** was then taken in dry DMF to which cetyl bromide (1.5 equivalent) and equivalent amount of K_2CO_3 were added. The solution was stirred at 80 °C for 24 h in an oil bath. EtOAc was added to the solution and washed with water to remove DMF. The organic layer was dried over sodium sulphate and column chromatography was performed in 60-120 mesh silica gel using chloroform/methanol as the eluent to obtain C-16 alkylated L-tyrosine at the –OH terminal (**II**).

Compound **II** was then dissolved in 3:1 methanol/chloroform (v/v) solution and stirred overnight with 1.1 equivalent of NaOH to hydrolyse the ester linkage. The organic solvents were removed and the reaction mixture taken in EtOAc was washed with excess dilute HCl to ensure conversion of the sodium salt of **III** to the neutral carboxylic acid. The organic layer was dried over sodium sulphate and evaporated in a rotary evaporator. The white solid residue was then purified by column chromatography using 60-120 mesh silica gel and chloroform/methanol as the eluent to obtain free –COOH terminal of O-alkylated and N-Boc protected tyrosine (**III**).

Acid terminal of intermediate **III** was then coupled with PEG using DCC (1 equiv) and a catalytic amount of DMAP in the presence of 1 equiv of HOBT in dry DCM. The amide was then purified through column chromatography using 60-120 mesh silica gel and chloroform/methanol as the eluent to obtain PEG linked **IV**. Intermediate **IV** was then subjected to deprotection by trifluoroacetic acid (1.5 equivalent) in dry DCM. After being stirred for 2 h, solvents were removed on a rotary evaporator and material was dried in a

vacuum pump. It was then dissolved in MeOH and treated with solid sodium carbonate. The organic part was filtered and concentrated to get the corresponding free amine (**V**).

NHS linked biotin was prepared by taking D-biotin (500 mg), DCC (1.5 equivalent) and NHS (1.1 equivalent) in dry DMF (8 mL) and stirred overnight under N₂ atmosphere. To this activated biotin (NHS-biotin) mixture, compound **V** and dry pyridine was added. The solution was stirred overnight and the DMF was distilled out under vacuum. The residue mixture was then purified using 100-200 mesh silica gel and chloroform/methanol as the eluent to obtain pure **1**.

Characterization of dispersing agents

¹H NMR of **1** (500 MHz, CDCl₃, Me₄Si, 25 °C) δ = 0.82-0.85 (m, 3H), 1.22-1.40 (m, 28H), 1.59-1.73 (m, 6H), 2.16-2.18 (m, 2H), 2.85-3.10 (m, 5H), 3.34 (s, 3H), 3.50-3.69 (m, 46H), 3.85-3.88(m, 2H), 4.23-4.24 (m, 2H), 4.29-4.31 (m, 1H), 4.49-4.50 (m, 1H), 4.78-4.80 (m, 1H), 6.75-6.77 (d, 2H), 7.01-7.02 (d, 2H). MS (ESI): m/z calculated for C₆₀H₁₀₇O₁₇N₃S: 1173.71; found: 1174.7133 [M + H⁺].

Preparation of SWNT-amphiphile dispersion

To an aqueous solution (4 mL) of **1** (2.5 mg/mL) SWNT (1 mg) was added. The solution was tip-sonicated for 30 min and bath sonicated for 2 h and again tip sonicated for 30 min. To remove the heavy bundles the solution was then centrifuged at 2500 g for 90 min. The amount of the dispersed SWNTs in the supernatant was calculated from the observed absorbance value at 550 nm that was derived from the previously reported calibration plot of absorbance versus concentration using sodium dodecylbenzene sulfonate.^{6h} The percentage dispersion was calculated as the ratio of the amount of SWNTs in the dispersion to the amount of SWNTs initially added.

TGA analysis:

The non-adsorbed amphiphile in the SWNT dispersion was removed by centrifugation. The obtained palette was dried in a vacuum oven. TGA thermogram of SWNT-1 composite was recorded by using a TA SDT Q600 instrument at a heating rate of 20 °C min under a N₂ atmosphere.

Sample preparation for ζ -potential, UV-vis-NIR, TEM and AFM

The aqueous SWNT suspension obtained after centrifugation at 2500 g was ultracentrifuged at 375000 g for 15 min. The supernatant was discarded to remove excess amphiphile **1** and the palette was redispersed in water (SWNT-1). The aqueous dispersion obtained was used for ζ -potential, UV-vis-NIR, TEM and AFM experiments. A drop of the SWNT suspension was placed on a 300-mesh Cu-coated TEM grid and dried under vacuum for 4 h before taking the image. Similarly in case of AFM studies, a drop of the dispersion was cast on a freshly cleaved mica surface and the samples were air-dried overnight before imaging. The bundle diameter was calculated from the height profile of the nanotubes. From 20 AFM images of SWNT-1 a statistical analysis of the bundle diameter and nanotube length was done by plotting histogram.

Cell culture

HepG2 and Hela cells were procured from National Center for Cell Science (NCCS), Pune (India), and HEK-293 and CHO cells were procured from ATCC and cultured in 10% FBS DMEM medium in presence of 100 mg/L streptomycin and 100 IU/mL penicillin. The cells were maintained in a 25 mL cell culture flask and kept at 37 °C in a humidified atmosphere of 5% CO₂ to about 70-80% confluence. Subculture was performed in every 2-3 days. The media was changed after 48-72 h to remove the dead cells. Subsequently the adherent cells

were detached from the surface of the culture flask by trypsinization. These cells were then used for cytotoxicity study as well as for internalization experiments of the SWNT-1 conjugates.

MTT Assay

Cell viability of the nanoconstructs was assessed by the microculture MTT reduction assay as previously reported.¹⁹ The assay involves the conversion of a soluble tetrazolium salt by mitochondrial dehydrogenase present in live cells to an insoluble colored product, formazan. The amount of formazan formed is estimated spectrophotometrically after dissolution of the product in DMSO. The amount of the formazan produced is proportional to the number of alive cells. The mammalian cells were seeded at a density of 15,000 cells per well in a 96-well microtiter plate 18-24 h before the assay. A stock solution of the SWNT-amphiphile dispersion was prepared in sterile water. Concentration of the nanohybrid in the microtiter plate was varied from 5 to 50 $\mu\text{g/mL}$. The cells were incubated with the nanoconstructs for 48 h at 37 °C under 5% CO_2 . The cells were further incubated for another 4 h in 15 μL MTT stock solution (5 mg/mL). The produced formazan was dissolved in DMSO and absorbance at 570 nm was measured using BioTek[®] Elisa Reader. The number of surviving cells were expressed as percent viability = $(A_{570}(\text{treated cells}) - \text{background}) / (A_{570}(\text{untreated cells}) - \text{background}) \times 100$.

Gel Electrophoresis

The gel for the electrophoresis was prepared by dissolving agarose (600 mg) in 20 mL of 1X Tris-boric acid-EDTA buffer. 2 μL of ethidium bromide (1 mg/mL) was added in that agarose solution during the preparation of the gel. A stock solution of SWNT-1 was prepared as mentioned above and that was diluted to prepare varying concentrations (25 $\mu\text{g/mL}$, 50 $\mu\text{g/mL}$ and 100 $\mu\text{g/mL}$) of solutions of (100 μL) of the nanoconjugate. The concentration was

determined using calibration plot. These solutions having varying concentration of SWNT-1 were separately incubated with 30 μM oligonucleotide solution (in Tris-EDTA pH=8 buffer) bearing the sequence ACCTGTGAGCCTTAC for 4 h at room temperature. Next the samples were mixed with 1 μL bromophenol blue (to track the oligonucleotide) taken in glycerol and loaded on to the above prepared agarose gel. Only oligonucleotide (30 μM) was also loaded onto the same gel as a standard. The gel was run at $E = 85 \text{ Vcm}^{-1}$ for 30 min and photographed by irradiating UV light. The band intensities were calculated with “quantity one” 1-D analysis software (Bio-Rad, Hercules, CA, USA).

Fluorescence Study

SWNT-1 (50 $\mu\text{g/mL}$) was mixed with fluorophore labeled Cy3-oligonucleotide (1.25 μM) for 4 h. At first the fluorescence intensity of only Cy3-Olg (1.25 μM) was measured by excitation at 550 nm and recording the 555-700 nm. Then the solution containing SWNT-1-Cy3-Olg was centrifuged at 175000 g to precipitate out SWNT-1-Olg conjugate as palette. Next the fluorescence intensity of the supernatant was recorded by exciting at same wavelength.

Preparation SWNT-1-Olg Conjugates

SWNT-1 (50 $\mu\text{g/mL}$) was mixed with the Cy3 tagged Olg (1.25 μM) and stirred for 4 h at room temperature to achieve the loading of the Cy3-Olg onto the SWNT surface. This SWNT-1-Cy3-Olg nanobioconjugate was diluted according to the requirement before incubation with different cells.

Incubation, Delivery and Imaging of Cells

Cy3-Olg loaded SWNT-1 suspensions were added into 24 well chambered plates containing confluent Hela, HepG2, HEK 293 and CHO cells in 10% FBS-DMEM culture media. The

concentration of SWNT in each well was 10 $\mu\text{g/mL}$ and the Cy3-Olg concentration was fixed at 0.25 μM . The final volume of the solution was 250 μL in each well. The nanobioconjugates were incubated with these cells for 3 h at 37°C in 5% CO_2 atmosphere. The cells were repeatedly washed with PBS buffer to ensure complete removal of the extracellular hybrids. The cells were then observed under the Olympus IX51 inverted microscope using an excitation filter BP530-550 and a band absorbance filter covering wavelength below 570 nm. Bright red images were observed when SWNT-1-Olg was internalized inside the cells. Similar cargo delivery experiments were carried out for HEK-293 and CHO cells in longer time scale (6-24 h) keeping all other conditions identical. The images were taken at 10x magnification.

Flow Cytometry

Required treated cells were suspended in 0.3 mL of PBS. Cells were analyzed using a flow cytometer, FACS Aria, operating at 560 nm excitation wavelength and at 530 \pm 30 nm detecting emission wavelength using a 500-570 nm bandpass filter for Cy3-Olg. The data was acquired and analyzed by 'Cell Quest' pro-software (Becton Dickinson, USA). Initially million cells were taken and the data was acquired from 10,000 cells. In case of the cell viability experiments the cells after treatment were stained with the LIVE/DEAD kit (Calcein and Ethidium Homodimer) for 30 min. The data was acquired using 488 nm (for live cells) and 585 nm (for dead cells).

Extraction of Doxorubicin from Doxorubicin Hydrochloride

Doxorubicin was extracted from a doxorubicin hydrochloride solution from a mixture of chloroform and pH 8.0 Tris EDTA buffer. Initially doxorubicin hydrochloride was dissolved in 100mL pH 8.0 Tris EDTA buffer having a composition of 0.1 M KCl, 40 mM tris(hydroxymethyl)aminomethane (Tris), 100 mM EDTA. Then 100 mL chloroform was

added to it and the biphasic mixture was vigorously stirred for 30 mins. The chloroform layer was separated and evaporated in vacuum to get pure doxorubicin.

Doxorubicin Loading

Doxorubicin was loaded onto SWNT-1 following a conventional protocol. To a dispersed solution of SWNT-1 in pH 8.0 PBS buffer having 100 $\mu\text{g/mL}$ SWNT, aqueous solution of doxorubicin was added such that the final concentration of doxorubicin in the conjugate is 50 $\mu\text{g/mL}$ and the mixture was kept overnight under stirring condition. UV-vis and fluorescence spectra of this hybrid material were checked with respect to control solutions having 100 $\mu\text{g/mL}$ SWNT and 50 $\mu\text{g/mL}$ doxorubicin concentration.

Targeted Delivery of Doxorubicin

The nanoconjugate SWNT-1-DOX was incubated with Hela and CHO cells for 12 h in cell seeded 96-well plates. The concentration of SWNT-1 was varied from 5 $\mu\text{g/mL}$ to 20 $\mu\text{g/mL}$ while the doxorubicin concentration was varied from 2.5 $\mu\text{g/mL}$ to 10 $\mu\text{g/mL}$. The concentration ratio of the nanovector : drug was maintained at 2:1 (w/w) throughout the experiment. The percentage of viable cells was determined using MTT assay as reported previously.

Acknowledgements

P.K.D. is thankful to CSIR, India (ADD, CSC0302) and DST, India (SR/S1/OC-25/2011) for financial assistance. S.B, M.G. and S.D. acknowledge CSIR, India for Research fellowships.

Electronic Supplementary Information (ESI)

TGA plot, suspension stability experiment, LIVE/DEAD images of Hela, HepG2 and CHO cells, structure reported amphiphile, control experiments with Cy3-Olg, amphiphile Cy3-Olg,

plot of surface tension versus concentration of amphiphile, energy depletion experiment, nuclear internalization experiment.

References.

1. (a) Z. Liu, K. Yang and S.T. Lee, *J. Mater. Chem.* 2011, **21**, 586; (b) F. Lu, L. Gu, M. J. Meziani, X. Wang, P. G. Luo, L. M. Veca, L. Cao and Y. P. Sun, *Adv. Mater.* 2009, **21**, 139; (c) Y. L. Wu, N. Putcha, K. W. Ng, D. T. Leong, C. T. Lim, S. C. J. Loo and X. Chen, *Acc. Chem. Res.* 2013, **46**, 782; (d) B. Wang, X. He, Z. Zhang, Y. Zhao and W. Feng, *Acc. Chem. Res.* 2013, **46**, 761.
2. (a) M. Prato, K. Kostarelos and A. Bianco, *Acc. Chem. Res.* 2008, **41**, 60; (b) S. Lee, M. G. Hahn, R. Vajtai, D. P. Hashim, T. Thurakitserree, A. C. Chipara, P. M. Ajayan and J. H. Hafn, *Adv. Mater.* 2012, **24**, 5261; (c) M. G. Hahn, A. L. M. Reddy, D. P. Cole, M. Rivera, J. A. Vento, J. Nam, H. Y. Jung, Y. L. Kim, N. T. Narayanan, D. P. Hashim, C. Galande, Y. J. Jung, M. Bundy, S. Karna, P. M. Ajayan and R. Vajtai, *Nano Lett.* 2012, **12**, 5616; (d) P. Chakravarty, R. Marches, N. S. Zimmerman, A. D. E. Swafford, P. Bajaj, I. H. Musselman, P. Pantano, R. K. Draper and E. S. Vitetta, *Proc. Natl. Acad. Sci.* 2008, **105**, 8697; (e) M. Ashokkumar, K. M. Sumukh, R. Murali, N. T. Narayanan, P. M. Ajayan and P. Thanikaivelan, *Carbon* 2012, **50**, 5572.
3. (a) B. L. Droumaguet, J. Nicolas, D. Brambilla, S. Mura, A. Maksimenko, L. D. Kimpe, E. Salvati, C. Zona, C. Airoidi, M. Canovi, M. Gobbi, M. Noiray, B. L. Ferla, F. Nicotra, W. Scheper, O. Flores, M. Masserini, K. Andrieux and P. Couvreur, *ACS Nano* 2012, **6**, 5866; (b) C. Kaewsaneha, P. Tangboriboonrat, D. Polpanich, M. Eissa and A. Elaissari, *ACS Appl. Mater. Interfaces* 2013, **5**, 1857; (c) Z. Su, S. Zhu, A. D. Donkor, C. Tzoganakis and J. F. Honek, *J. Am. Chem. Soc.* 2011, **133**, 6874; (d) S. T. Kim, K. Saha, C. Kim and V. M. Rotello, *Acc. Chem. Res.* 2013, **46**, 681; (e) N. W. S. Kam, M. O. Connell, J. A. Wisdom and

H. Dai, *Proc. Natl. Acad. Sci.* 2005, **102**, 11600; (f) C. Bussy, H. A.; Boucetta and K. Kostarelos, *Acc. Chem. Res.* 2013, **46**, 692.

4. (a) D. Pantarotto, R. Singh, D. M. Carthy, M. Erhardt, J. P. Briand, M. Prato, K. Kostarelos and A. Bianco, *Angew. Chem. Int. Ed.* 2004, **43**, 5242; (b) A. P. Goodwin, S. M. Tabakman, K. Welsher, S. P. Sherlock, G. Prencipe and H. Dai, *J. Am. Chem. Soc.* 2009, **131**, 289; (c) R. Singh, D. Pantarotto, L. Lacerda, G. Pastorin, C. Klumpp, M. Prato, A. Bianco and K. Kostarelos, *Proc. Natl. Acad. Sci.* 2006, **103**, 3357; (d) N. Nakayama- Ratchford, S. Bangsaruntip, X. Sun, K. Welsher and H. Dai, *J. Am. Chem. Soc.* 2007, **129**, 2448; (e) M. Benincasa, S. Pacor, W. Wu, M. Prato, A. Bianco and R. Gennaro, *ACS Nano* 2011, **5**, 199.

5. (a) D. Das and P. K. Das, *Langmuir* **2009**, **25**, 4421-4428; (b) H. Xie, A. O. Acevedo, V. Zorbas, R. H. Baughman, R. K. Draper, I. H. Musselman, A. B. Dalton and G. R. Dieckmann, *J. Mater. Chem.*, 2005, **15**, 1734; (c) C. G. Salzmann, M. A. H. Ward, R. M. J. Jacobs, G. Tobias and M. L. H. Green, *J. Phys. Chem. C* 2007, **111**, 18520; (d) E. J. Becraft, A. S. Klimenko and G. R. Dieckmann, *Peptide Sci.* 2009, **92**, 212; (e) C. Backes, C. D. Schmidt, K. Rosenlehner, F. Hauke, J. N. Coleman and A. Hirsch, *Adv. Mater.* 2010, **22**, 788; (f) S. Dutta, T. Kar, S. Brahmachari and P. K. Das, *J. Mater. Chem.* 2012, **22**, 6623; (g) V. Georgakilas, K. Kordatos, M. Prato, D. M. Guldi, M. Holzinger and A. Hirsch, *J. Am. Chem. Soc.* 2002, **124**, 760; (h) B. G. Cousins, A. K. Das, R. Sharma, Y. Li, J. P. McNamara, I. H. Hillier, I.A. Kinloch and R. V. Ulijn, *Small* 2009, **5**, 587; (i) E. Schopf, R. Broyer, L. Tao, Y. Chen and H. D. Maynard, *Chem. Commun.* 2009, 4818; (j) L. Shao, G. Tobias, C. G. Salzmann, B. Ballesteros, S. Y. Hong, A. Crossley, B. G. Davis and M. L. H. Green, *Chem. Commun.* 2007, 5090; (k) A. D. Crescenzo, D. Demurtas, A. Renzetti, G. Siani, P. D. Maria, M. Meneghetti, M. Prato and A. Fontana, *Soft Matter* 2009, **5**, 62; (l) C. Backes, C. D. Schmidt, F. Hauke, C. Bottcher and A. Hirsch, *J. Am. Chem. Soc.* 2009, **131**, 2172; (m) Y. Li, B. G. Cousins, R. V. Ulijn and I. A. Kinloch, *Langmuir* 2009, **25**, 11760.

6.(a) N. W. S. Kam and H. Dai, *J. Am. Chem. Soc.* 2005, **127**, 6021; (b) M. A. Herrero, J. Guerra, V. S. Myers, M. V. Gomez, R. M. Crooks and M. Prato, *ACS Nano* 2010, **4**, 905; (c) M. Ahmed, N. Bhuchar, K. Ishihara and R. Narain, *Bioconjugate Chem.* 2011, **22**, 1228; (d) Z. Liu, M. Winters, M. Holodniy and H. Dai, *Angew. Chem. Int. Ed.* 2007, **46**, 2023; (e) N. W. S. Kam, T. C. Jessop, P. A. Wender, and H. Dai, *J. Am. Chem. Soc.* 2004, **126**, 6850; (f) N. W. S. Kam, Z. Liu and H. Dai, *J. Am. Chem. Soc.* 2005, **127**, 12492; (g) C. Richard, N. Mignet, C. Largeau, V. Escriou, M. Bessodes and D. Scherman, *Nano Res.* 2009, **2**, 638; (h) S. Brahmachari, D. Das and P. K. Das, *Chem. Commun.* 2010, **46**, 8386; (i) Z. Liu, X. Li, S. M. Tabakman, K. Jiang, S. Fan and H. Dai, *J. Am. Chem. Soc.* 2008, **130**, 13540; (j) Z. Liu, X. Sun, N. N. Ratchford and H. Dai, *ACS Nano* 2007, **1**, 50; (k) D. Pantarotto, J.-P. Briand, S. Muller, M. Prato and A. Bianco, *Nat. Nanotechnol.* 2007, **2**, 108 (l) N. W. S. Kam, Z. Liu and H. Dai, *Angew. Chem. Int. Ed.* 2006, **45**, 577.

7. S. Brahmachari, D. Das, A. Shome and P. K. Das, *Angew. Chem. Int. Ed.* 2011, **50**, 11243.

8. (a) S. Park, H. S. Yang, D. Kim, K. Job and S. Jon, *Chem. Commun.* 2008, 2876; (b) Z. Liu, K. Chen, C. Davis, S. Sherlock, Q. Cao, X. Chen and H. Dai, *Cancer Res.* 2008, **68**, 6652; (c) T. Maldiney, C. Richard, J. Seguin, N. Wattier, M. Bessodes and D. Scherman, *ACS Nano* 2011, **5**, 854; (d) S.T. Yang, K. A. S. Fernando, J. H. Liu, J. Wang, H.F. Sun, Y. Liu, M. Chen, Y. Huang, X. Wang, H. Wang, Y.P. Sun, *Small* 2008, **4**, 940; (e) G. Prencipe, S. M. Tabakman, K. Welsher, Z. Liu, A. P. Goodwin, L. Zhang, J. Henry and H. Dai, *J. Am. Chem. Soc.* 2009, **131**, 4783; (f) L. Lacerda, M. A. Herrero, K. Venner, A. Bianco, M. Prato, and K. Kostarelos *Small* 2008, **4**, 1130.

9.(a) J. Chen, S. Chen, X. Zhao, L. V. Kuznetsova, S. S. Wong and I. Ojima, *J. Am. Chem. Soc.* 2008, **130**, 16778; (b) S. Dhar, Z. Liu, J. Thomale, H. Dai and S. J. Lippard, *J. Am. Chem. Soc.* 2008, **130**, 11467; (c) Z. Liu, C. Davis, W. Cai, L. He, X. Chen and H. Dai, *Proc. Natl. Acad. Sci.* 2008, **105**, 1410; (d) R. P. Feazell, N. N. Ratchford, H. Dai and S. J. Lippard,

J. Am. Chem. Soc. 2007, **129**, 8438; (e) S. Chen, X. Zhao, J. Chen, J. Chen, L. Kuznetsova, S. S. Wong and I. Ojima, *Bioconjugate Chem.* 2010, **21**, 979; (f) A. A. Bhirde, V. Patel, J. Gavard, G. Zhang, A. A. Sousa, A. Masedunskas, R. D. Leapman, R. Weigert, J. S. Gutkind and J. F. Rusling, *ACS Nano* 2009, **3**, 307; (g) X. Zhang, L. Meng, Q. Lu, Z. Fei and P. J. Dyson, *Biomaterials* 2009, **30**, 6041; (h) C. Zhang, S. Gao, W. Jiang, S. Lin, F. Du, Z. Li and W. Huang, *Biomaterials* 2010, **31**, 6075.

10. I. Ojima, *Acc. Chem. Res.* 2008, **41**, 108.

11.(a) L. G. Lis, M. A. Smart, A. Luchniak, M. L. Gupta, Jr. and V. J. Gurchich, *ACS Med. Chem. Lett.*, 2012, **3**, 745; (b) G. Russell-Jones, K. McTavish, J. McEwan, J. Rice and D. Nowotnik, *J. Inorg. Biochem.* 2004, **98**, 1625; (c) W. Yang, Y. Cheng, T. Xu, X. Wang and L. Wen, *Eur. J. Med. Chem.* 2009, **44**, 862; (d) S. Y. Kim, S. H. Cho and Y. M. Lee, *Macromol. Res.* 2007, **15**, 646.

12. J. Orczyk, D. M. Morr'e and D. Morr'e1 *J. Mol. Cell. Biochem.* 2005, **273**, 161.

13. S. Attal, R. Thiruvengadathan and O. Regev, *Anal. Chem.*, 2006, **78**, 8098.

14.(a) X. Wang, T. Xia, S. A. Ntim, Z. Ji, S. George, H. Meng, H. Zhang, V. Castranova, S. Mitra and A. E. Nel, *ACS Nano*, 2010, **4**, 7241; (b) B. Zhao, H. Hu, A. Yu, D. Perea and R. C. Haddon, *J. Am. Chem. Soc.* 2005, **127**, 8197.

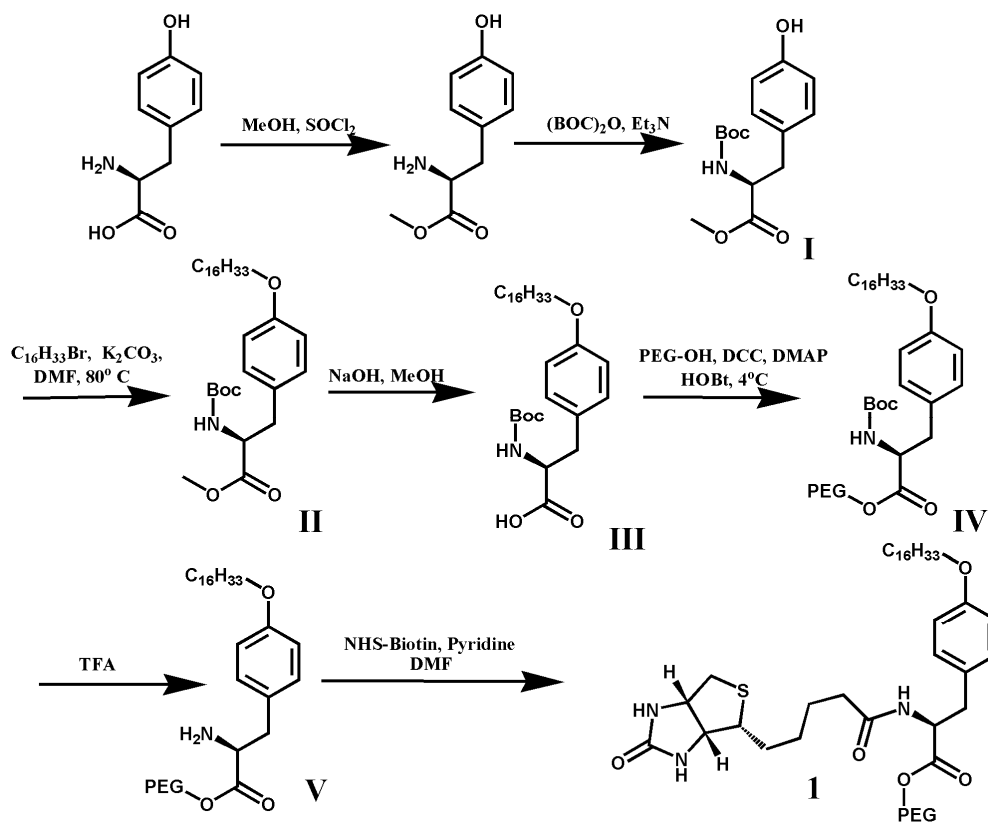
15. L. S. Witus, J. D. R. Rocha, V. M. Yuwono, S. E. Paramonov, R. B. Weismana and J. D. Hartgerink, *J. Mater. Chem.*, 2007, **17**, 1909.

16. R. Gref, M. Lu'ck, P. Quellec, M. Marchand, E. Dellacherie, S. Harnisch, T. Blunk and R.H. Mu"ller, *Colloids Surf. B*, 2000, **18**, 301.

17. (a) R. Singh, D. Pantarotto, D. McCarthy, O. Chaloin, J. Hoebeke, C. D. Partidos, J. P. Briand, M. Prato, A. Bianco and K. Kostarelos, *J. Am. Chem. Soc.* 2005, **127**, 4388; (b) D. W. Chang, I. Y. Jeon, J. B. Baek and L. Dai, *Chem. Commun.* 2010, **46**, 7924

18.(a) H. A. Boucetta, K. T. A. Jamal, D. McCarthy, M. Prato, A. Bianco and K. Kostarelos, *Chem. Commun.* 2008, 459; (b) X. Yang, X. Zhang, Z. Liu, Y. Ma, Yi. Huang and Y. Chen, *J. Phys. Chem. C*, 2008, **112**, 17554.

19. M. B. Hansen, S. E. Nielsen and K. Berg, *J. Immunol. Methods*, 1989, **119**, 203.



Scheme 1. Synthetic scheme of **1**; PEG = -(CH₂CH₂O)₁₂CH₃

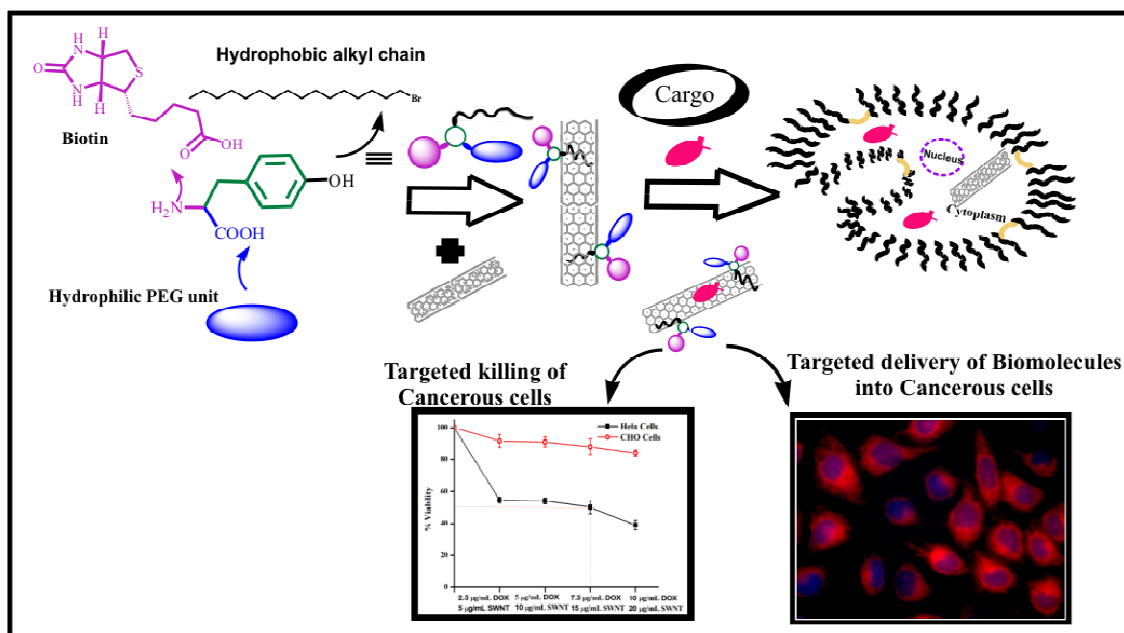


Fig. 1 Pictorial representation on specific delivery of drug and biomolecule loaded SWNT-biotinylated amphiphile nanoconjugate into cancer cells.

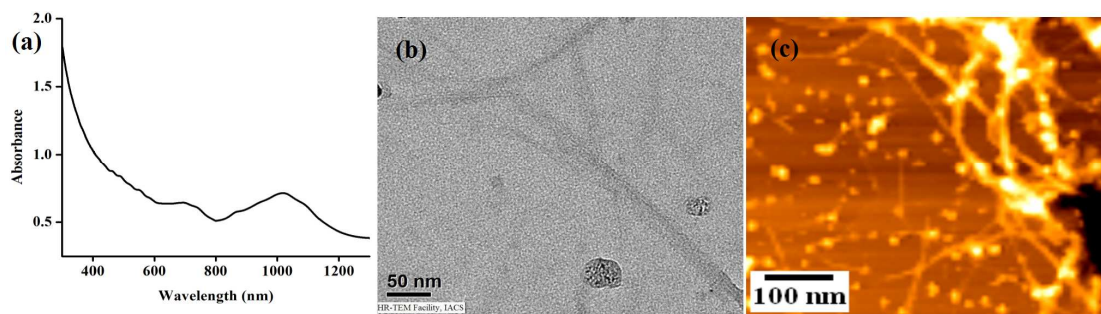


Fig. 2 a) UV/vis/NIR spectra of aqueous SWNT-1 dispersion b) TEM images of SWNT-1 nanohybrid and c) AFM images of SWNT-1 nanohybrid.

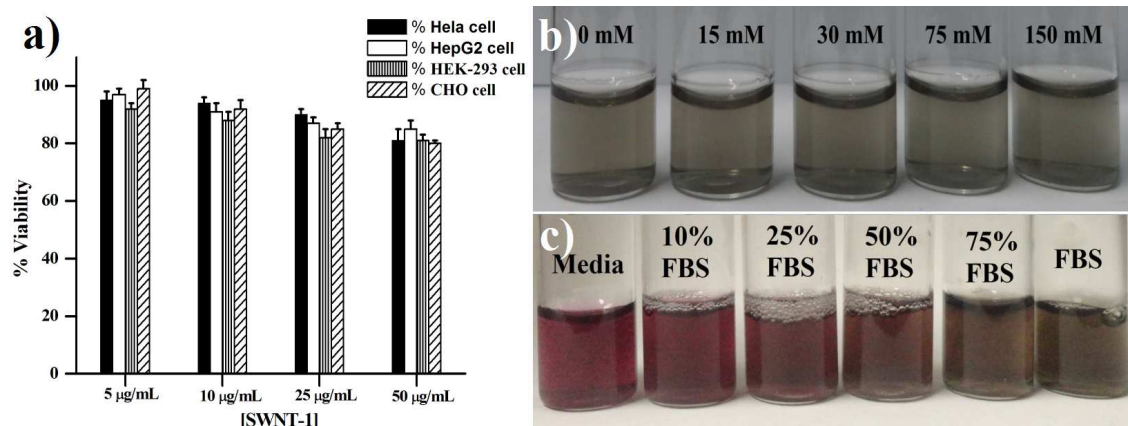


Fig. 3 (a) Viability of HeLa, HepG2, HEK-293 and CHO cells treated with varying concentrations of SWNT-1 nano hybrids for 48 h. Percent errors are within $\pm 5\%$ in triplicate experiments. . Photographs of vials after incubating 25 $\mu\text{g}/\text{mL}$ SWNT-1 for 48 h in (b) solutions of varying concentration of PBS and (c) with varying FBS concentrations in DMEM media.

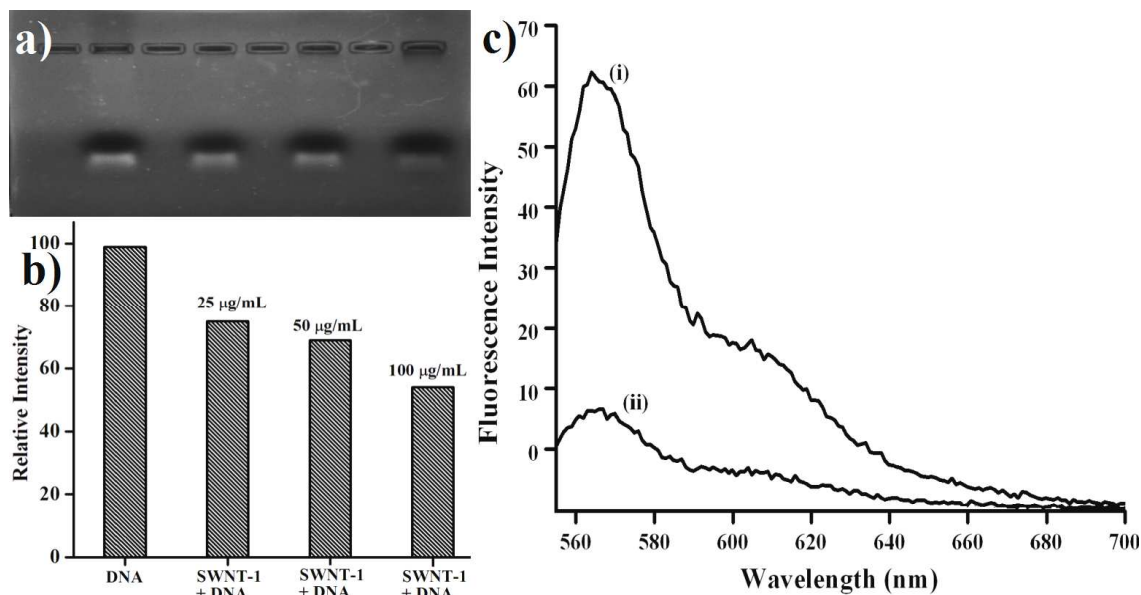


Fig. 4 (a) Photograph of UV radiated agarose gel after migration of SWNT-complexed and free oligonucleotide (b) Relative intensities i) oligonucleotide (30 μM), ii) SWNT-1 (25 $\mu\text{g/mL}$)-Olg (30 μM), iii) SWNT-1 (50 $\mu\text{g/mL}$)-Olg (30 μM), iv) SWNT-1 (100 $\mu\text{g/mL}$)-Olg (30 μM) (c) fluorescence spectra of (i) Cy3-Olg (1.25 μM) (ii) supernatant solution after precipitation of SWNT-1 (50 $\mu\text{g/mL}$)-Cy3-Olg (1.25 μM) nanohybrid.

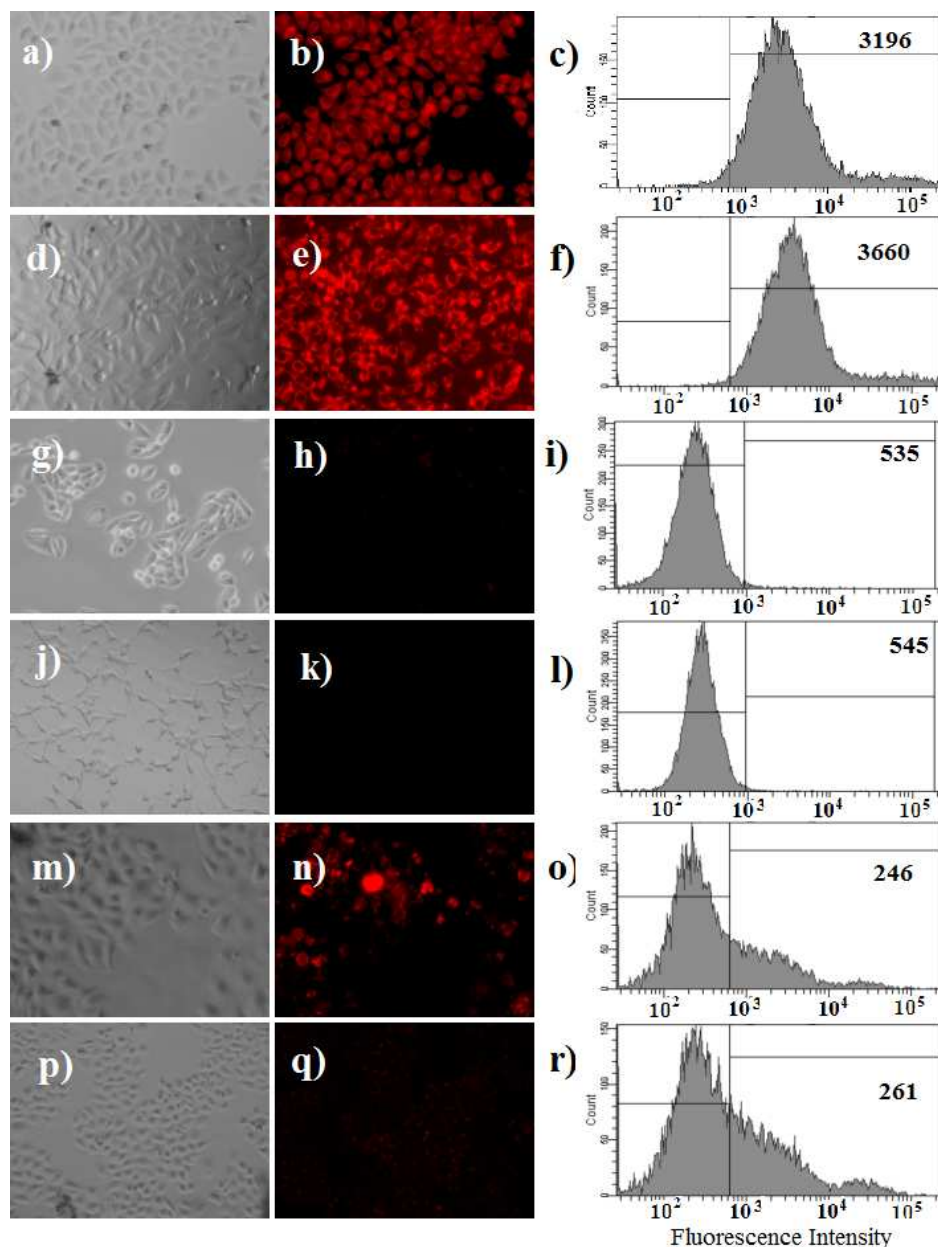


Fig. 5 Microscope images (a,d,g,j,m,p: bright field; b,e,h,k,n,q: fluorescence) of cells incubated for 3 h with Cy3-Olg loaded SWNT-1 a,b) HeLa cells, c) corresponding flow cytometric data for HeLa cells d,e) HepG2 cells, f) corresponding flow cytometric data for HepG2 cells, g,h) CHO cells, i) corresponding flow cytometric data for CHO cells, j,k) HEK-293, l) corresponding flow cytometric data for HEK-293 cells, m,n) biotin pretreated HeLa Cells, o) corresponding flow cytometric data for biotin pretreated HeLa cells, [nanoconjugate] = 10 $\mu\text{g}/\text{mL}$ and [Cy3-Olg] = 0.25 μM . p,q) internalization with SWNT-amphipile without biotin in HeLa cells. [nanoconjugate] = 10 $\mu\text{g}/\text{mL}$ and [Cy3-Olg] = 0.25 μM , r) corresponding flow cytometric data. In all the flow cytometry plot the x-axis denotes the fluorescence intensity. The mean fluorescence values are given in the inset and that of unstained control cells = 97.

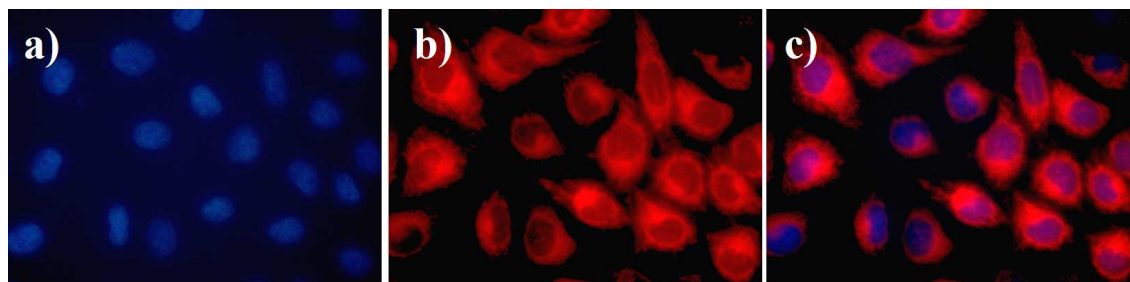


Fig. 6 (a) HeLa cells stained with Hoechst dye after incubation of cells for 3 h with Cy3-Olg loaded SWNT-1, (b) internalized of the Cy3-Olg into the cytoplasm of HeLa cells up on 3 h incubation with Cy3-Olg loaded SWNT-1, (c) superimposed image of a and b.

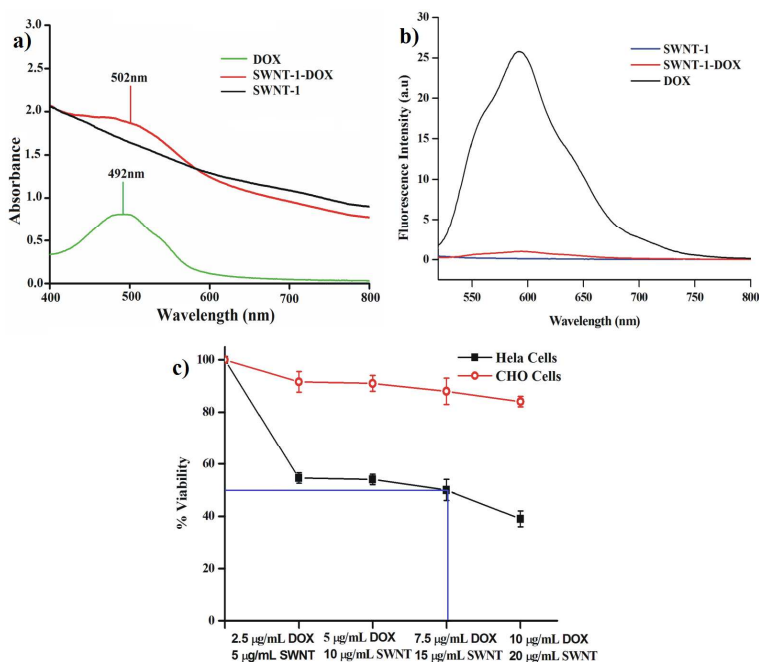
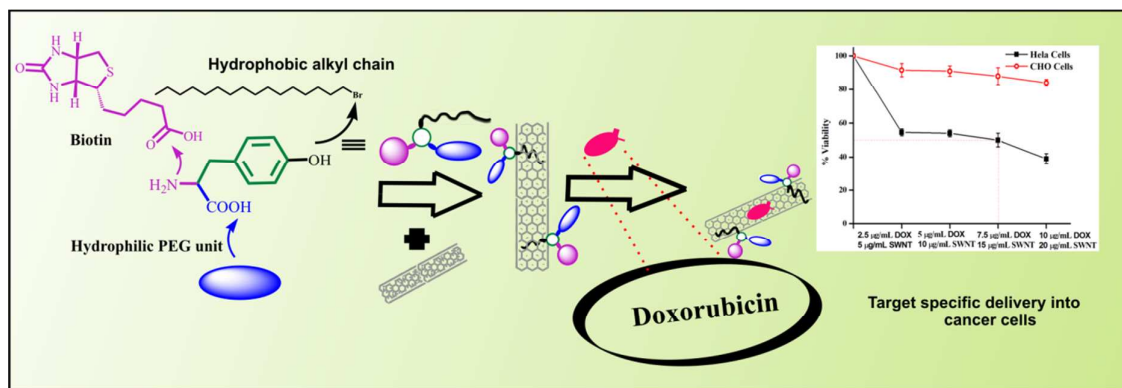


Fig. 7 (a) UV-vis spectra of doxorubicin, SWNT-1-DOX and SWNT (b) fluorescence spectra of doxorubicin, SWNT-1-DOX and SWNT . (c) cell viability of HeLa and CHO cells treated with varying concentrations of SWNT-1-DOX nano hybrids for 12 h. Percent errors are within $\pm 5\%$ in triplicate experiments.

Graphical contents



The present work reports the development of an amino acid based trifunctionalized biotinylated SWNT dispersing agent for target-specific delivery. SWNT-amphiphile hybrid exhibited receptor-mediated specific delivery of biomolecule and anticancer drug to cancer cells (Hela, HepG2) in contrast to non-cancerous cells (HEK-293 and CHO).